Calculation of electron scattering from the ground state of barium

Dmitry V. Fursa* and Igor Bray
Electronic Structure of Materials Centre, The Flinders University of South Australia, G.P.O. Box 2100, Adelaide 5001, Australia
(Received 29 July 1998)

We present nonrelativistic convergent close coupling calculations of electron scattering from the ground state of barium at energies ranging from 1 to 987 eV. At selected energies the effect of the inclusion or neglect of the target continuum is estimated. Very good agreement is found with measurements of the $(6s6p)\ ^1P^o$ apparent cross section at all energies. In addition, good agreement is obtained for differential cross sections of elastic scattering, and $(6s6p)\ ^1P^o$ and $(6s5d)\ ^1D^e$ excitations. The calculated $(6s6p)\ ^1P^o$ electron-photon angular correlations are in good agreement with experiment. [S1050-2947(98)05212-3]

PACS number(s): 34.80.Bm, 34.80.Dp

I. INTRODUCTION

This decade has seen immense progress in the calculation of electron-atom scattering. To a large extent this is due to the computational technology, particularly with large random-access memory (RAM), that has become recently available. In our case the change in computational technology has changed the direction of research. In the previous decade we concentrated on numerical techniques that required relatively small RAM [coupled-channels optical (CCO) method [1]], whereas now using the convergent close-coupling (CCC) method we work routinely with large-scale ($15\,000\times15\,000$) matrices requiring machines in excess of 1 Gb of RAM.

The CCC method was developed in response to the long-standing discrepancy between theory and experiment for the 54.4-eV $2P$ angular correlation parameters at backward angles, but failed to resolve this discrepancy [2]. However, recently Yalim, Cvejanovic, and Crowe [3] reported new measurements which yielded excellent agreement with theory where previous measurements did not. Furthermore, O'Neill *et al.* [4] also reported new measurements claiming the corresponding older ones were in error, though their data did not support the theory quite as well as those of Yalim, Cvejanovic, and Crowe. Further support to theory has been given by Williams [5] who discusses the difficulty of the measurements and gives new measurements at the lower energy of 16.5 eV, where the $2P$ cross section is substantially larger at the backward angles than at 54.4 eV, and finds excellent agreement with theory.

From the theoretical standpoint the above e-H scattering problem has become primarily an experimental one. Now, we would argue, the major fundamental problem between theory and experiment is the substantial discrepancy in magnitude for the e-He(2^3S) excitation to higher triplet states [6]. The CCC results have been recently confirmed by Bartschat [7] while the experimental data has been recently reanalyzed and further increase the discrepancy [8,9].

We are confident in the accuracy of the CCC method for electron scattering from ground states of light atoms with one or two valence electrons. It has been successfully applied to H, He, Be, Li, and Na atoms [2,10–13]. It has always been our aim to develop the method into a general electron-atom–ion scattering theory, capable of providing reliable data for a large variety of targets. The extension we are presently investigating is application of the CCC method to heavier targets, but only those with one or two valence electrons. The barium atom is an ideal choice due the availability of extensive and detailed experimental data.

Over the past two decades electron-barium scattering has been subject of intense experimental and theoretical study. Foundation for detailed experimental study of e-Ba scattering processes has been established with accurate measurement of the $(6s6p)\ ^1P^o$ apparent cross section by Chen and Gallagher [14]. Although the cascade contributions to the direct $(6s6p)\ ^1P^o$ cross section at low and intermediate energies have been only roughly estimated, it was used for absolute normalization of the elastic $(6s6p)\ ^1P^o$ and $(6s5d)\ ^1D^e$ differential cross sections (DCSs) by Jensen, Register, and Trajmar [15], and later for elastic and $(6s6p)\ ^1P^o$ DCSs by Wang, Trajmar, and Zetner [16]. The total ionization cross section has been measured by Vainshtein *et al.* [17] and Dettmann and Karstensen [18]. The total cross section was measured by Romanyuk, Shpenik, and Zapesochny [19].

One of the most attractive properties of the barium atom is that the $(6s6p)\ ^1P^o$ level can be pumped from the ground state using readily available lasers. The first measurements of electron scattering DCSs from excited states of barium, the $(6s6p)\ ^1P^o$ level and the $(6s5d)\ ^1D^e$ metastable level, have been reported by Register *et al.* [20]. More recently, cross sections for scattering from the $(6s6p)\ ^1P^o$ state of barium have been reported by Li and Zetner [21], Zetner *et al.* [22], and Trajmar *et al.* [23]. Laser excitation of the $(6s6p)\ ^1P^o$ level allows for measurement of electron impact coherence parameters (EICPs) [24] for this level using the superelastic scattering technique. This way EICPs have been measured for the $(6s6p)\ ^1P^o$-$(6s5d)\ ^1D^e$ transition by Li and Zetner [25], and for the $(6s6p)\ ^1P^o$-$(6s^2)^1S$ transition by Zetner, Li, and Trajmar [26,27] and Li and Zetner [28]. In addition, EICPs were obtained for the elastic $(6s6p)\ ^1P^o$-$(6s6p)\ ^1P^o$ transition by Trajmar *et al.* [23].

Measurement of electron scattering from excited states of barium are of great importance for both practical applications [29–31] and for testing fundamental aspects of

*Electronic address: Dmitry.Fursa@flinders.edu.au

electron-atom scattering theory. They pose a serious challenge to existing theoretical methods. To date only the unitarized distorted wave approximation (UDWA) calculations have been extensively applied to the problem [22,32], while the CCC method has been applied to the calculation of the elastic $(6s6p)\ ^1P^o$-$(6s6p)\ ^1P^o$ transition [23] and the $(6s6p)\ ^1P^o$-$(6s5d)\ ^1D^e$ transition [33].

On the other hand scattering from the ground state has been studied theoretically in much more detail. Gregory and Fink [34] solved numerically the Dirac equation with a relativistic Hartree-Fock-Slater potential and presented elastic scattering results at 100–1500 eV. Szmytkowski and Sienkiewicz [35] have used the relativistic polarized-orbital approximation for the calculation of elastic scattering from 0.2 to 100 eV. The two- and three-state close-coupling calculations of Fabrikant [36–38] are nonrelativistic calculations which used semiempirical target wave functions. The results of the two-state $(6s^2)^1S$ and $(6s6p)\ ^1P^o$ calculations [37], which neglect exchange between the projectile and the target electrons, have been reported at many energies.

Excitation of the $(6s6p)\ ^1P^o$ state has been studied by Clark *et al.* [39] using unitarized distorted-wave approximation. This method incorporates relativistic mass and Darwin corrections and one-body spin-orbital term in the calculation of the Ba wave functions, but no relativistic corrections have been included in the projectile-target potential. Srivastava *et al.* used the relativistic distorted-wave approximation (RDWA) to calculate cross sections and EICPs for excitation of the lowest lying $^{1,3}P_1$ states [40] and the $^{1,3}D_{1,2,3}$ states [41]. The RDWA is a fully relativistic method both in the calculation of the target structure and the electron scattering, based on the solution of the Dirac equations.

The important conclusion from both the UDWA and RDWA calculations is that for the singlet $(6s6p)P$ and $(6s5d)D$ state excitations the relativistic effects, both in calculation of the target structure and electron scattering, are negligible. This was also supported by the experimental results of Li and Zetner [28] for the degree of polarization P for the $(6s6p)^1P^o$ state, which was found to be equal to unity, in accordance with nonrelativistic theory. We, therefore, feel confident that the CCC method, which presently is nonrelativistic, can provide valuable and reliable information for the large spin-preserving transitions. For the ground initial state these involve elastic scattering and the excitation of the $(6s6p)^1P^o$ and $(6s5d)^1D^e$ states.

Recently we have applied the CCC method to investigate electron scattering from the ground state of barium at the single incident electron energy of 20 eV [42]. The purpose of this paper is to expand on this work and present detailed analysis of *e*-Ba scattering across a wide range of incident electron energies.

In Sec. II we will provide details of the calculation of the barium wave functions and electron scattering. This is followed by a detailed comparison of our results with experiment and earlier calculations. We also discuss the breakdown of the nonrelativistic approximation for excitation of the $(6s6p)^3P_1^o$ and $(6s5d)^3D_2^e$ states and indicate how it can be remedied. Finally, in Sec. IV, we formulate conclusions and indicate future direction for our research.

II. BARIUM WAVE FUNCTION AND ELECTRON SCATTERING CALCULATIONS

The detailed description of the CCC method for calculation of electron scattering from alkaline earth atoms has been given and demonstrated by application to *e*-Be scattering [11]. The extension to barium from beryllium is straightforward.

The calculation of the Ba target structure is performed in the nonrelativistic LS coupling scheme. For the Ba structure we use a model of two valence electrons above an inert Hartree-Fock core. Configuration-interaction (CI) expansion (for valence electrons) is used to calculate target wave functions. A self-consistent Hartree-Fock calculation is performed for the Ba^+ ion. The $1s$, $2s$, $2p$, $3s$, $3p$, $3d$, $4s$, $4p$, $4d$, $5s$, and $5p$ orbitals are then frozen and used to define the frozen-core Hartree-Fock Hamiltonian H_1. We obtain a further set of single-particle orbitals by diagonalization of the Ba^+ ion (one-electron) Hamiltonian H_1 in a Laguerre basis. The radial parts of the single-particle functions are

$$\xi_{kl}(r)=\left(\frac{\lambda_l(k-1)!}{(2l+1+k)!}\right)^{1/2}\times(\lambda_l r)^{l+1}\exp(-\lambda_l r/2)L_{k-1}^{2l+2}(\lambda_l r), \tag{1}$$

where the $L_{k-1}^{2l+2}(\lambda_l r)$ are the associated Laguerre polynomials, and k ranges from 1 to the basis size N_l.

This calculation has been performed in two steps [11]. The first diagonalization is performed to obtain good excited Ba^+ orbitals. The typical Laguerre basis parameters N_l,λ_l used were $N_0=33,\lambda_0=5$, $N_1=33,\lambda_1=5$, $N_2=30,\lambda_2=4$, and $N_3=25,\lambda_3=3$. The second diagonalization uses the $n\leqslant 5$ core orbitals, together with $n\leqslant 6$ frozen-core Hartree-Fock [43] orbitals, and the $n\geqslant 7$ orbitals obtained from the first diagonalization, to obtain an orthonormal set of orbitals which describes the ground and the excited states of Ba^+ well.

A phenomenological core-polarization potential $V^{\rm pol}$ has been added to H_1 in order to fit the one-electron ionization energies of the Ba^+ ion. This potential is chosen to be the same as in Ref. [13],

$$V^{\rm pol}(r)=-\frac{\alpha_d}{2r^4}\,W_6(r/\rho_l), \tag{2}$$

where

$$W_m(r/\rho)=1-\exp[-(r/\rho)^m], \tag{3}$$

and α_d is the static dipole polarizability of the core. We use the following values for the dipole polarizability: $\alpha_d=11$ a.u. and cutoff radii $\rho_0=1.8$, $\rho_1=2.2$, $\rho_2=3.4$, and $\rho_3=2.47$ a.u.

The two-electron configurations have been chosen in such a way that one of the electrons always occupies one of the $6s$, $7s$, $6p$, $7p$, or $5d$ orbitals (ionic core orbitals) of the Ba^+ ion. We have found that this set of orbitals is sufficient to account for the electron-electron correlations in the low-lying target states. We have added a phenomenological two-electron polarization potential [44,45] to the electron-electron Coulomb potential

TABLE I. Ionization energies for low-lying states in barium. Experimental data from Moore [63] and Palenius [64] ($5d^{23}F^e$ and $5d^{21}S$ levels). States are labeled by the major configuration.

	Experiment		Present			Experiment		Present	
	Label	E (eV)	Label	E (eV)		Label	E (eV)	Label	E (eV)
^1S	$6s^2$	5.211	$6s^2$	5.237	^3S	$6s7s$	1.968	$6s7s$	1.962
	$5d^2$	1.894	$5d^2$	1.899		$6s8s$	1.008	$6s8s$	0.841
	$6s7s$	1.711	$6s7s$	1.687		$5d6d$	0.693	$5d6d$	0.627
	$6p^2$	0.950	$6s8s$	0.734	$^3P^o$	$6s6p$	3.589	$6s6p$	3.649
$^1P^o$	$6s6p$	2.972	$6s6p$	2.973		$6p5d$	2.008	$6p5d$	1.941
	$5d6p$	1.671	$6s7p$	1.625		$6s7p$	1.380	$6s7p$	1.367
	$6s7p$	1.176	$6s8p$	1.099		$7p5d$	0.606	$7p5d$	0.543
	$6s8p$	0.761	$6s9p$	0.507	$^3D^e$	$6s5d$	4.051	$6s5d$	4.026
$^1D^e$	$6s5d$	3.798	$6s5d$	3.798		$6s6d$	1.396	$6s6d$	1.386
	$5d^2$	2.352	$5d^2$	2.214		$7s5d$	1.097	$7s5d$	1.077
	$6s6d$	1.462	$6s6d$	1.448		$6s7d$	0.777	$5d6d$	0.698
	$7s5d$	1.021	$7s5d$	1.028	$^3F^o$	$6p5d$	2.349	$6p5d$	2.357
	$6p^2$	0.829	$6s7d$	0.708		$6s4f$	0.919	$6s4f$	0.897
$^1F^o$	$6p5d$	1.887	$6p5d$	1.893		$6s5f$	0.567	$6s5f$	0.414
	$6s4f$	0.905	$6s4f$	0.881	$^3P^e$	$5d^2$	2.274	$5d^2$	2.129
	$6s5f$	0.589	$7p5d$	0.576		$6p^2$	0.844	$6p^2$	0.694
	$7p5d$	0.532	$6s5f$	0.371	$^3D^o$	$6p5d$	2.152	$6p5d$	2.126
$^1P^e$	$5d6d$	0.636	$5d6d$	0.664		$7p5d$	0.603	$7p5d$	0.599
$^1D^o$	$6p5d$	2.350	$6p5d$	2.368	$^3F^e$	$5d^2$	2.616	$5d^2$	2.456
	$7p5d$	0.614	$7p5d$	0.636		$5d6d$	0.561	$5d6d$	0.525
			$5d4f$	0.208	$^1F^e$	$5d6d$	0.727	$5d6d$	0.717

$$V_{12}^{\mathrm{d}}(\hat{\boldsymbol{r}}_1\cdot\hat{\boldsymbol{r}}_2)=-\frac{\alpha_d}{r_1^2 r_2^2}P_1(\hat{\boldsymbol{r}}_1\cdot\hat{\boldsymbol{r}}_2)\sqrt{W_6(r_1/\rho)W_6(r_2/\rho)}, \tag{4}$$

where P_1 is the Legendre polynomial of degree 1, $\rho=4.4$ a.u., and the value of $\alpha_d=11$ a.u. is the same as in Eq. (2). The parameter ρ of this potential has been obtained to achieve best agreement with the experimental values for the $(6s6p)^1P^o$ and $(6s5d)^1D^e$ energy levels. We thus obtain at least three bound states (if any) for each target symmetry sufficiently accurately.

The ionization energy levels for low-lying states of barium are given in Table I. For triplet states the experimental values have been obtained by weighted averaging over fine-structure sublevels. We also give the state label corresponding to the major configuration in the CI expansion. Agreement with experiment is quite good. Our results are similar to those of Friedrich and Trefftz [46] who also used a nonrelativistic CI method.

In Table II we compare our results for oscillator strengths f with experiment and other calculations. Present results have been calculated using the modified form of the dipole length operator [44,47]. In the nonrelativistic formalism the oscilla-

TABLE II. Oscillator strength (a.u.) for selected transitions in Ba.

	Present	Calculations	Experiments
$(6s6p)^1P^o$-$(6s^2)^1S$	1.686	2.136 [22], 1.68 [49]	1.59 [65], 1.64 [66]
$(6s7p)^1P^o$-$(6s^2)^1S$	0.122	0.161 [22], 0.14 [49]	0.174 [65], 0.14 [67]
$(5d^2)^1S$-$(6s6p)^1P^o$	0.006	0.033 [46]	
$(6s7s)^1S$-$(6s6p)^1P^o$	0.185	0.153 [46]	
$(5d^2)^1D^e$-$(6s6p)^1P^o$	0.085	0.1 [46]	
$(6s6p)^1P^o$-$(6s5d)^1D^e$	0.0035	0.0019 [22], 0.0057 [49]	$\leqslant$ 0.0034 [68]
$(6s7p)^1P^o$-$(6s5d)^1D^e$	0.118	0.122 [22], 0.13 [49]	0.13 [69], 0.17 [70]
$(6p5d)^1F^o$-$(6s5d)^1D^e$	0.158	0.346 [22], 0.2 [49]	0.39$\pm$50% [51]
$(6s4f)^1F^o$-$(6s5d)^1D^e$	0.116	0.25 [46]	0.25 [51]$\pm$50%, 0.12 [71]
$(6s4f)^3D^o$-$(6s5d)^3D^e$	0.365	0.41 [46], 0.51 [72]	0.66$\pm$50% [51]
$(6p5d)^3P^o$-$(6s5d)^3D^e$	0.256	0.32 [46], 0.25 [72]	0.45$\pm$50% [51]
$(6p^2)^3P^e$-$(6s6p)^3P^o$	0.529	0.63 [46], 0.47 [72]	0.77$\pm$50% [51]
$(6s6p)^3P_1^o$-$(6s5d)^3D_1^e$	0.013	0.0089 [22], 0.017 [49]	0.0154$\pm$25% [51]
$(6s6p)^3P_1^o$-$(6s5d)^3D_2^e$	0.023	0.0135 [22], 0.029 [49]	0.0263$\pm$25% [51]

tor strength for transition between states of different multiplicity is zero. For transitions between triplet states we present multiplet average values. For transitions between components of multiplet we assume LS coupling and express the oscillator strength via the multiplet average value (see Sobel'man [48] for details)

$$f(^{2S'+1}L'_{J'};{}^{2S+1}L_J)=(2L+1)(2J'+1)\times\begin{Bmatrix} S' & J & L \\ 1 & L' & J' \end{Bmatrix}^2\times\delta_{S',S}f(^{2S'+1}L';{}^{2S+1}L). \quad (5)$$

Here initial (final) state has spin S (S'), orbital angular momentum L (L'), and total angular momentum J (J'). Generally, our results are in good agreement with experiment and other accurate calculations. The last two entries in the table make use of Eq. (5) as specific J and J' are given. Excellent agreement with the $(6s6p)^3P_1^o$-$(6s5d)^3D_{1,2}^e$ lines, which have a relatively small experimental uncertainty, suggests that singlet-triplet mixing for these levels is small. This is supported by the results of Bauschlicher, Jr. *et al.* [49] for the $(6s6p)^3P_1^o$ level who gave the value of the mixing parameter $\sin\beta=0.0919$ in the equation

$$\Phi'((6s6p)^3P_1^o)=\cos\beta\,\Phi((6s6p)^3P_1^o)-\sin\beta\,\Phi((6s6p)^1P_1^o). \quad (6)$$

We have used in Eq. (6) the nonrelativistic Russell-Saunders wave functions in the $LSJM$ representation via

$$\Phi^{JLS\Pi}_{m_J}=\sum_{m_L,m_S}C^{LSJ}_{m_Lm_Sm_J}\Phi^{LS\Pi}_{m_Lm_S}, \quad (7)$$

where Π is the parity. The singlet-triplet mixing for the $(6s5d)^3D_2^e$ state can be accounted for in a similar manner,

$$\Phi'((6s5d)^3D_2^e)=\cos\beta\,\Phi((6s5d)^3D_2^e)-\sin\beta\Phi((6s5d)^1D_2^e), \quad (8)$$

with value of mixing parameter $\cos\beta=0.978$ taken from the calculations by Trefftz [50].

Following Bauschlicher, Jr. *et al.* [49] we can use Eq. (6) in order to estimate the oscillator strength for the intercombination line $(6s6p)^3P_1^o$-$(6s^2)^1S$. Our value of 0.00998 a.u. is in good agreement with the experimental value of 0.00994 a.u. $\pm 50\%$ [51]. Although singlet-triplet mixing for the $(6s6p)^3P_1^o$ and $(6s5d)^3D_2^e$ levels is small, we will see in the next section that it is sufficient to break down the nonrelativistic approximation for electron impact excitation of these levels. In this case we may remedy, in an approximate way, this problem using Eqs. (6) and (8).

For the ground state we have calculated the static dipole polarizability using oscillator strengths for ^1P states. Both negative energy and positive energy states have been used. The obtained value of $264.3a_0^3$ is in very good agreement with the recommended value of $(268\pm 21.6)a_0^3$ quoted by Miller and Bederson [52]. The dominant part of the polarizability (92%) comes from the resonance $(6s6p)^3P_1^o$ level. The continuum contributes less than 1%. This is in contrast to the case of helium, where approximately half of the polarizability is due to the continuum.

Barium wave functions exhibit a great deal of configuration interaction, not only in the low-lying states but also for the high-lying discrete spectrum states. A better accuracy in the description of the high-lying states is achieved by simply increasing the size of the Laguerre basis. However, this leads to a very fine discretization of the target continuum, requiring unnecessarily large close-coupling calculations. Instead we form optimized orbitals suitable for the low-lying states and have the Ba continuum predominantly based on the Ba^+ ground states core, just as we did for the case of the Be target [11].

The e-Ba scattering calculations have been performed in two models. The first has only negative-energy states (relative to the Ba^+ ground state) included in the close-coupling expansion. This, 55-state, close-coupling calculation [CC(55)] comprises five ^1S, six $^1P^o$, seven $^1D^e$, five $^1F^o$, three ^3S, six $^3P^o$, five $^3D^e$, five $^3F^o$, one $^1P^e$, three $^1D^o$, one $^1F^e$, three $^3P^e$, three $^3D^o$, and two $^3F^e$ states. The second, 115-state calculation [CCC(115)], has both negative- and positive-energy states. This close-coupling calculation comprises of 14 ^1S, 17 $^1P^o$, 19 $^1D^e$, 19 $^1F^o$, 7 ^3S, 9 $^3P^o$, 9 $^3D^e$, 9 $^3F^o$, and two each of $^{1,3}P^e$, $^{1,3}D^o$, $^{1,3}F^e$ states. The negative energy states in CC(55) and CCC(115) calculations are exactly the same for first three states of each symmetry, while differing insignificantly for most of the higher lying negative energy states. The difference in the results of the scattering calculations in these two models should come from the coupling to the ionization continuum which is absent in the CC(55) calculations and present in the CCC(115) calculations. The CC(55) calculations take significantly less computer time. We therefore have chosen to perform CC(55) calculations over a wide energy range, while CCC(115) calculations have been performed at selected incident electron energies. Note, that no attempt has been made in the present work to reproduce resonance behavior of the cross section in the interval between first excitation threshold and ionization threshold. The present technique is not the most efficient method for such purposes, other methods, most notably the R-matrix method [53,54], is a more convenient choice in this case.

III. RESULTS

The great strength of the close-coupling method is that from a single calculation for a given total energy we obtain scattering amplitudes between all states included in the calculation. Thus, elastic, excitation, and ionization processes are calculated simultaneously from the ground and excited states. On the other hand, the calculations are particularly exhaustive of the computational resources. For this reason it is particularly helpful to have experiments, which usually concentrate on a single transition, to be performed at the same total energy where measurements exist for other transitions. This way a single calculation may be tested against a wider range of experiments that may involve scattering from the ground or excited states.

Given the large set of results that the CCC calculations yield we separate their discussion into three subsections. The

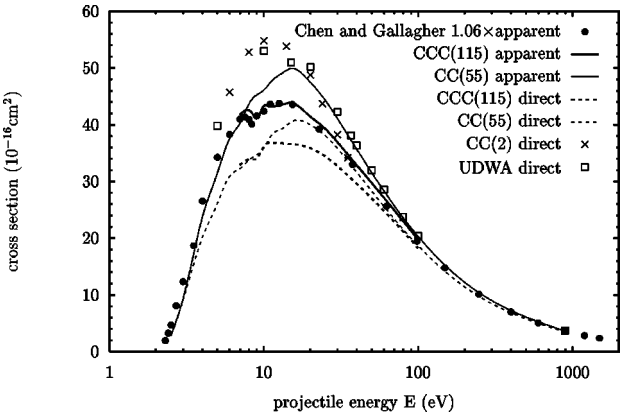

FIG. 1. Apparent and direct $6\,^1P^o$ excitation integrated cross sections for electron scattering from the Ba ground state. The CCC(115) and CC(55) calculations are described in the text. The UDWA calculations are due to Clark *et al.* [39] and CC(2) calculations are due to Fabrikant [37]. The experiment due to Chen and Gallagher [14], has been renormalized by the factor of 1.06, see text.

first subsection deals with integrated cross sections, the second with differential cross sections, and the third with electron-photon angular correlations for the $(6s6p)^1P^o$ state.

A. Integrated cross sections

The integrated cross section (ICS) for the $(6s6p)^1P^o$ level is of particular importance because it is used for the normalization of elastic and other excitation cross sections. No measurements of the direct $(6s6p)^1P^o$ ICS are available to date. Chen and Gallagher [14] reported measurements of the optical excitation function which is the sum of the direct $(6s6p)^1P^o$ ICS and cascade contribution from the higher lying levels. We have calculated branching ratios for the Ba negative energy states and used them together with the ICS from the CCC(115) and CC(55) calculations to evaluate cascade contributions and hence estimate the measured optical excitation function. Both direct and apparent cross sections from the CCC(115) and CC(55) calculations are presented in Fig. 1. The direct cross section results of the two-state close-coupling calculations of Fabrikant [37] and the UDWA calculations of Clark *et al.* [39] are also presented.

We see that above the ionization threshold (5.2 eV) the apparent cross section measurements are substantially below the results of the CC(55) calculations. Below the ionization threshold excellent agreement is found at 5 and 4 eV, but at lower energies, where there is no cascading contribution, we find our results to be somewhat below the experimental data.

Comparing the CCC(115) and CC(55) ''apparent'' results we find that the inclusion of the coupling to the ionization continuum reduced the cross section to the experimental values, after the latter has been multiplied by 1.06. The reason for the renormalization is that the Chen and Gallagher data was normalized at high energy to the Born result of Kim and Bagus [55]. At 897 eV our Born value is 3.63×10^{-16} cm^2 (with 4.6% cascade contribution) and the Born value of Kim and Bagus is 3.41×10^{-16} cm^2 (with 4% cascade contribution). The corresponding oscillator strength in our calculations is 1.69 which is identical to the value calculated by Bauschlicher, Jr. *et al.* [49], who suggest that the most accurate experimental estimate is 1.64 ± 0.16. Therefore, we suspect that a marginally more accurate normalization of the experiment is achieved by multiplying the experiment by 1.06, the ratio of the two Born results.

Interesting to note that the experimentally observed structure in the apparent cross section at 8.35 eV is absent in the CC(55) results but is present in the CCC(115) results, where the total ionization cross section has a sharp maximum, see Fig. 8. We believe that the origin of the structure in the experimental excitation function at 8.35 eV is caused by relative diminishing of both the direct cross section and the cascade contribution to it due to a loss of flux to ionization channels.

Comparing the different theories for the direct ICS, assuming the CCC(115) to be the most accurate, we see that the two-state results of Fabrikant [37] and the UDWA results of Clark *et al.* [39] are substantially too high. However, the RDWA results of Srivastava *et al.* [40] (not presented) are even larger. The major difference between the UDWA and RDWA results comes from the unitarization procedure used in the UDWA calculation. Our work has demonstrated that accurate ICS at the intermediate energies are only able to be obtained if coupling is allowed to higher discrete states and the target continuum.

The present results are tabulated in Table III. The cascade contribution to the apparent $(6s6p)^1P^o$ ICS for the CCC(115) calculations is smaller than in the CC(55) calculations. Loss of flux to the ionization channels in the CCC(115) model is responsible for this. As the incident electron energy increases the results of the two models converge to the Born approximation. We find that the majority ($>80\%$) of the cascade contribution comes from the excitation of the $(5d^2)^1D$, $(6s6d)^1D$, $(6p^2)^1D$, $(6s7s)^1S$, and $(6s8s)^1S$ states. All of these have a branching ratio of ≈1, except for $(6p^2)^1D$ which has a branching ratio of ≈0.8. At incident electron energy of 5, 10, 15, and 20 eV our estimate of the cascade contribution to the $(6s6p)^1P^o$ optical excitation function (see Table III) is different from the values of 5% at 5 eV, 10% at 10 and 15 eV, and 20% at 20 eV used by Wang, Trajmar, and Zetner [16] for the normalization of the differential cross sections (DCSs). It is also substantially different from the cascade estimate of 30% by Jensen, Register, and Trajmar [15] which was used for the normalization of the DCS at 20 to 100 eV energies. Accordingly, we believe these should be marginally renormalized for greater accuracy.

In Fig. 2 we present comparison of the experimental and theoretical results for the polarization of the Ba $6\,^1P^o$ line. The influence of the barium isotope mixture (18% of ^{135}Ba and ^{137}Ba with nuclear spin I=3/2) on the polarization function has been discussed by Fabrikant [37]. We use Eq. (12) from Ref. [37],

$$P=\frac{\sigma_0-\sigma_1}{1.104\sigma_0+1.210\sigma_1}, \tag{9}$$

where σ_m, $m=0,1$ are magnetic sublevel integrated cross sections. We have calculated polarization fraction P in the four (55-, 115-state apparent and direct) cases. We consid-

TABLE III. CCC(115) and CC(55) apparent ICS for the $(6s6p)^1P^o$ state and the cascade contribution in percentage.

	CC(55)		CCC(115)			CC(55)		CCC(115)	
Energy (eV)	ICS (10^{-16} cm^2)	(%)	ICS (10^{-16} cm^2)	(%)	Energy (eV)	ICS (10^{-16} cm^2)	(%)	ICS (10^{-16} cm^2)	(%)
2.5	2.8	0.0			20.	47.5	15.8	41.4	13.2
3	9.3	0.0			21.44	46.6	15.2	40.5	12.8
4	23.8	15.0			30	41.1	12.9		
5	31.5	17.1			36.67	37.3	11.8	34.1	10.4
6	37.6	17.6			41.44	35.0	11.2	32.4	9.8
7	40.2	19.9	41.8	21.4	50	31.6	10.3		
8.35	44.5	23.4	42.1	19.2	60	28.3	9.6		
9	45.3	23.4	41.1	17.1	80	23.6	8.6		
10	46.1	22.1	43.4	16.7	100	20.23	8.0	19.3	6.7
11.44	48.0	19.8	43.2	14.8	200	12.2	6.6		
13	49.0	19.9			897.6	3.63	4.6		
15	50.0	18.9	43.9	15.0					

ered radiation from each magnetic sublevel of the cascading states to the magnetic sublevels of the $(6s6p)^1P^o$ state, but found that cascading did not affect the polarization noticeably. Similarly, both CC(55) and CCC(115) models are essentially the same and are in very good agreement with experiment over the energy range. The CC(2) calculations of Fabrikant [37] are in fair agreement with experiment. The conclusion from this comparison is that taking just a few discrete states is sufficient for describing the polarization function.

Our results for elastic scattering are presented in Fig. 3. The upper plot gives the ICS and lower plot gives the momentum transfer cross section. We find very good agreement between CCC(115) and CC(55) for both cross sections, as well as good agreement with the experimental data of Wang, Trajmar, and Zetner [16] and Jensen, Register, and Trajmar [15]. Principal features of the elastic ICS and momentum transfer cross section are similar. The depression in our results at around 10 eV is caused by a deep minimum in the $L=3$ partial wave cross section. At incident electron energies larger than 30 eV the optical potential model (OPM) calculations of Kelemen, Remeta, and Sabad [56] are in good agreement with our results. The two-state results of Fabrikant [37] are in a fair agreement with our results, but differ somewhat in shape and absolute values.

The results of the present calculations for $(6s5d)^1D^e$ ICS are presented in Fig. 4. Good agreement is found with the measurements of Jensen, Register, and Trajmar [15]. Generally, we are confident in the accuracy of the CCC calculations for the spin-preserving transitions, excitation of singlet states in the present case, to an accuracy of $\pm 10\%$. Some uncertainty comes into the CCC calculations from the effect

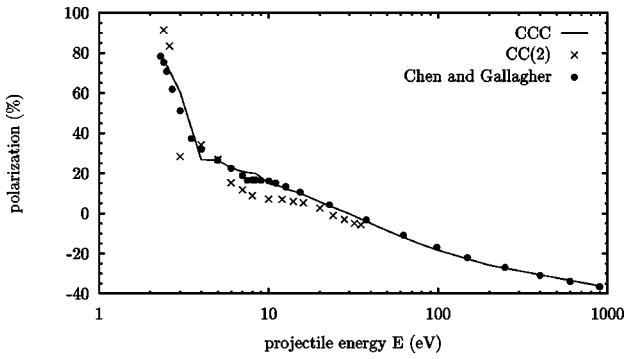

FIG. 2. Polarization of the barium $6\,^1P^o$ line. Calculations and experiment are as for Fig. 1, except that the single curve labeled CCC denotes the result of our four [CCC(115), CC(55) direct, and cascade, see text], barely distinguishable in the present case calculations.

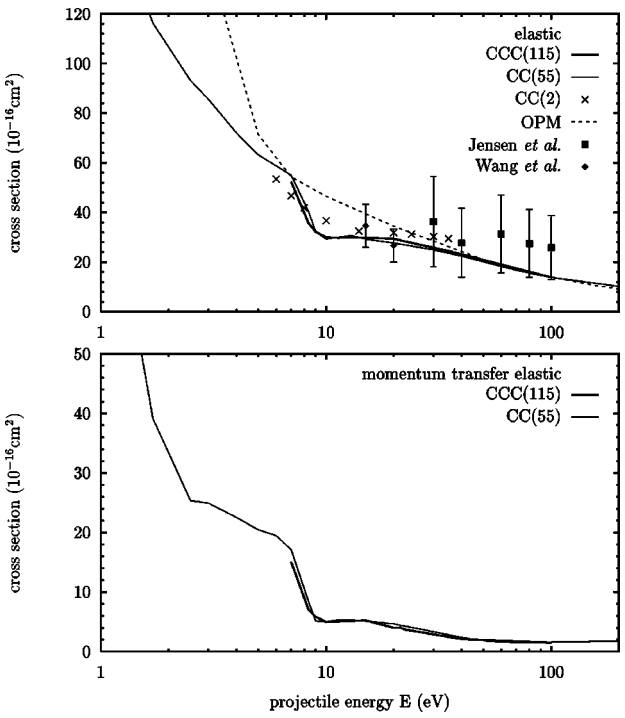

FIG. 3. Integrated and momentum transfer cross sections for *e*-Ba elastic scattering. Calculations are as for Fig. 1, in addition the optical potential model (OPM) calculation is due to Kelemen, Remeta, and Sabad [56]. Measurements are due to Jensen, Register, and Trajmar [15] and Wang, Trajmar, and Zetner [16].

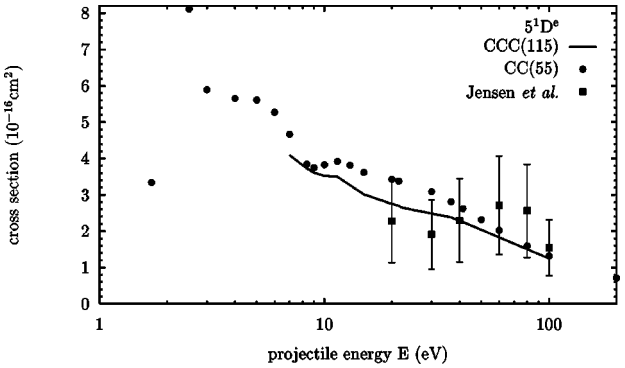

FIG. 4. Integrated cross sections for the e-Ba $5\,{}^1D^e$ excitation. Calculations are as for Fig. 1. Measurements are due to Jensen, Register, and Trajmar [15].

of pseudoresonances and internal numerical stability due to the size of the matrices involved.

We now consider two transitions where the final state is a triplet state and relativistic corrections are expected to be important. In Fig. 5 we present our results for $(6s6p)^3P^o$ and $(6s5d)^3D^e$ ICS. In the nonrelativistic approximation the cross section $\sigma(^{2S+1}L_J)$ for the excitation of the fine-structure component J is related to the cross section for the excitation of the total multiplet $\sigma(^{2S+1}L)$,

$$\sigma(^{2S+1}L_J)=\frac{(2J+1)}{(2S+1)(2L+1)}\sigma(^{2S+1}L). \qquad (10)$$

While this relation should be quite accurate for excitation of $(6s6p)^3P^o_{0,2}$ and $(6s5d)^3D^e_{1,3}$ sublevels, the singlet-triplet mixing can considerably affect the $(6s6p)^3P^o_1$ and the $(6s5d)^3D^e_2$ cross sections. Using Eqs. (6) and (8) we can estimate the effect of the singlet-triplet mixing on the

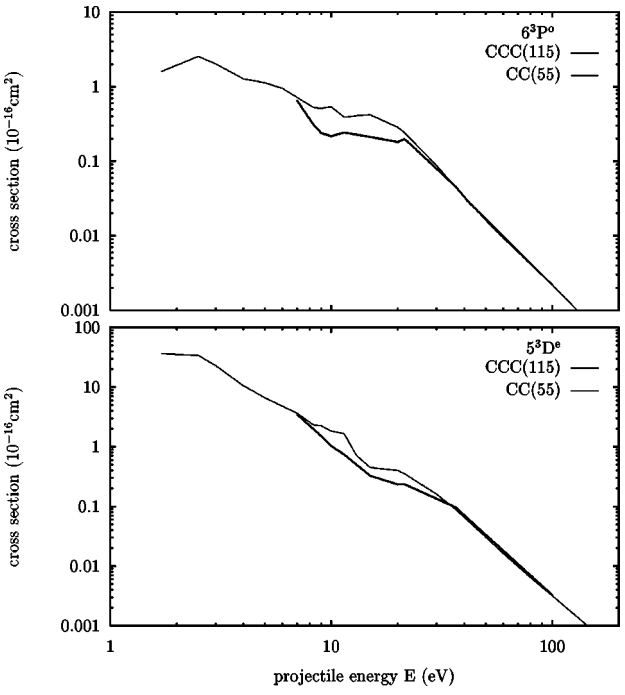

FIG. 5. Integrated cross sections for the e-Ba $6\,{}^3P^o$ and $5\,{}^3D^e$ excitation. Theoretical calculations are as for Fig. 1.

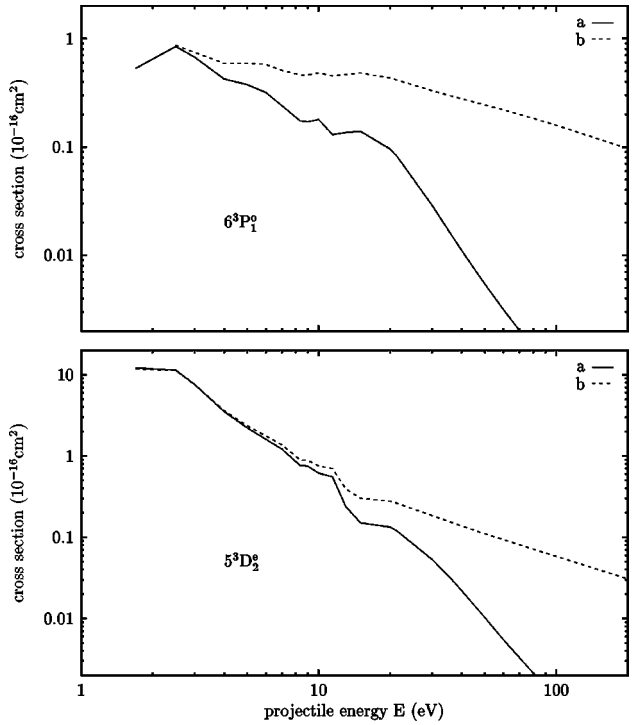

FIG. 6. Integrated cross sections for the e-Ba $6\,{}^3P^o_1$ and $5\,{}^3D^e_2$ excitations. The curve labeled a is the result of the nonrelativistic CC(55) calculations, the curve labeled b accounts for singlet-triplet mixing and breakdown of the nonrelativistic model, see text for details.

$(6s6p)^3P^o_1$ and $(6s5d)^3D^e_2$ excitation cross sections. These (fine structure) cross sections are found to be

$$\sigma_{\rm fs}(^3P^o_1)=\frac{1}{3}\cos^2\beta\sigma(^3P^o)+\sin^2\beta\sigma(^1P^o), \qquad (11)$$

$$\sigma_{\rm fs}(^3D^e_2)=\frac{1}{3}\cos^2\beta\sigma(^3D^o)+\sin^2\beta\sigma(^1D^e), \qquad (12)$$

and are presented in Fig. 6 together with the uncorrected triplet results. Interesting to note that in both cases considered here, the combination of the corresponding singlet and triplet amplitudes results in the cancellation of the interference terms, and leads to a relation involving only cross sections in Eqs. (11) and (12).

From the figure we see that there is a large increase in the ICS as the incident electron energy decreases, with $(6s5d)^3D^e$ ICS becoming the largest excitation cross section below 4 eV. The cross sections (11) and (12), and cross sections for excitation of the $(6s6p)^3P^o_1$ and $(6s5d)^3D^e_2$ fine-structure sublevels [see Eq. (10)] are presented in Fig. 6 for CC(55) calculations. Clearly, a completely nonrelativistic model for the $(6s6p)^3P^o_1$ level becomes inadequate as incident electron energy increases a few eV above the excitation threshold. This is due to the fact that there is a large increase of the ratio of the singlet P excitation cross to the triplet P one, which easily offsets the small singlet-triplet mixing coefficient. Similarly to the excitation of the $(6s6p)^1P^o_1$ state, the behavior of the cross section will be predetermined by the value of the optical oscillator strength for the intercombination $(6s6p)^3P^o_1$-$(6s^2)^1S$ line which is in good agreement with experiment, see Eq. (6). Singlet-triplet mixing for

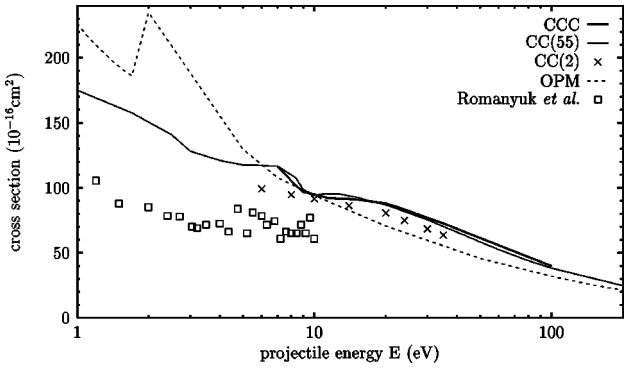

FIG. 7. Total cross section for electron scattering from the Ba ground state. Theoretical calculations as in Fig. 1. Experiment is due to Romanyuk, Spernik, and Zapesochny [19].

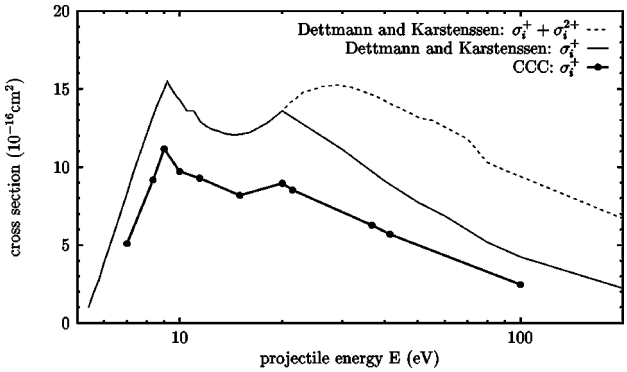

FIG. 8. Total ionization cross section for electron scattering on the Ba ground state. Theoretical calculations are as for Fig. 1. Experiment is due to Dettmann and Karstenssen [18].

the $(6s5d)^3D_2^e$ level affects scattering results in a somewhat different manner. The reason for this is the large cross section for the excitation of the triplet *5D* state relative to the singlet *5D* state as compared with singlet and triplet *6P* excitation cross sections. We find, therefore, that singlet-triplet mixing for the $(6s5d)^3D_2^e$ level becomes important at incident electron energies above 10 eV.

In Fig. 7 we compare total cross section (TCS) experimental data of Romanyuk, Shpenik, and Zapesochny [19] with our CCC(115) and CC(55) results. The results of the CC(2) calculation by Fabrikant [37] and OPM calculation by Kelemen, Remeta, and Sabad [56] are also presented. We find very good agreement between our CCC(115) and CC(55) calculations. The CC(2) calculations of Fabrikant [37] are in fair agreement with our results. This indicates that convergence of close-coupling expansion is achieved relatively fast for the TCS. The OPM results are in poor agreement with our results at low energies, though agreement improves as incident electron energy increases. Unfortunately, agreement with absolute measurements of TCS by Romanyuk, Spernik, and Zapesochny [19] is very poor at low energies. Given the very good agreement of our calculations with 6^1P^o optical excitation function measurements [14] and with experimental estimates of the elastic ICS [16], we believe that the theoretical results are more reliable.

The CCC(115) calculations provide estimate of the total ionization cross section (TICS). We compare our results with experiment of Dettmann and Karstenssen [18] for single and double electron ionization, σ_i^+ and σ_i^{2+}, in Fig. 8. We refer to Dettmann and Karstenssen [18] for references and comparison with other theories and experiments. Our CCC results do not account for any contribution from double ionization and should be compared with σ_i^+ data of Dettmann and Karstenssen [18]. We find that our results substantially underestimate experimental σ_i^+ data, however, are in quite good shape agreement with experiment (σ_i^+ data). This is somewhat unexpected because at least at low energies the CCC model should account for all major ionization processes, including ionization with residual Ba^+ ion excitations. We performed more calculations at selected energies with the inclusion of *G* states which resulted in at most a 10% increase in the cross sections. The convergence in the TICS, with increasing target-space orbital angular momentum, is relatively fast [57]. Thus we believe the presented results are possibly around 10% lower than the true results calculated using a much larger close-coupling basis. Interesting to note that such a correction would bring our results to be in very good agreement with the TICS measurements of Vainshtein *et al.* [17] in the 7–11.4 eV energy interval. The maximum value for the TICS (at 9 eV) read from Fig. 2 of Vainshtein *et al.* [17] is 12.1*e*-16 cm^2 while present CCC result plus 10% is 12.3*e*-16 cm^2.

B. Differential cross sections

In Figs. 9, 10, and 11 we present comparison between theoretical calculations and experimental measurements for elastic, $(6s6p)^1P^o$ and $(6s5d)^1D^e$ DCS at incident electron energies from 5 to 100 eV. The relative experimental mea-

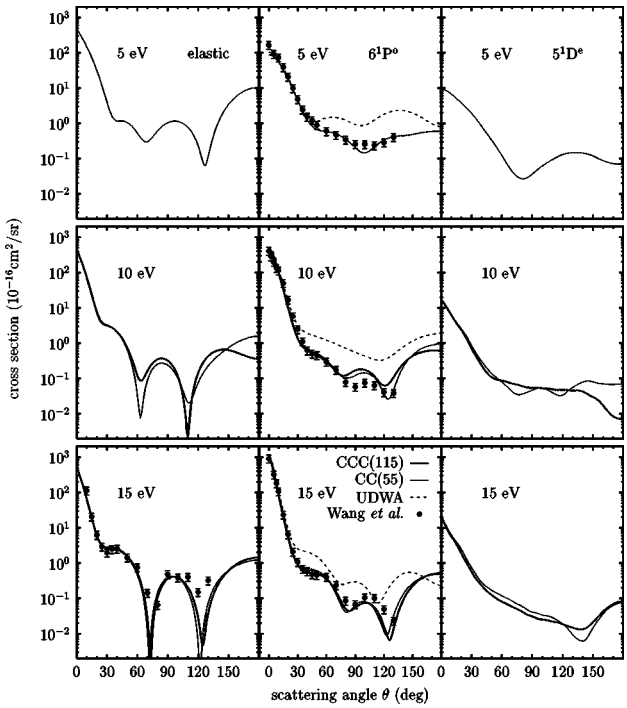

FIG. 9. The elastic, 6^1P^o, and 5^1D^e excitation differential cross section for electron scattering on the Ba ground state at 5, 10, and 15 eV incident electron energy. The CCC(115) and CC(55) calculations are described in the text. The UDWA calculations are due to Clark *et al.* [39]. The measurements are due to Wang, Trajmar, and Zetner [16].

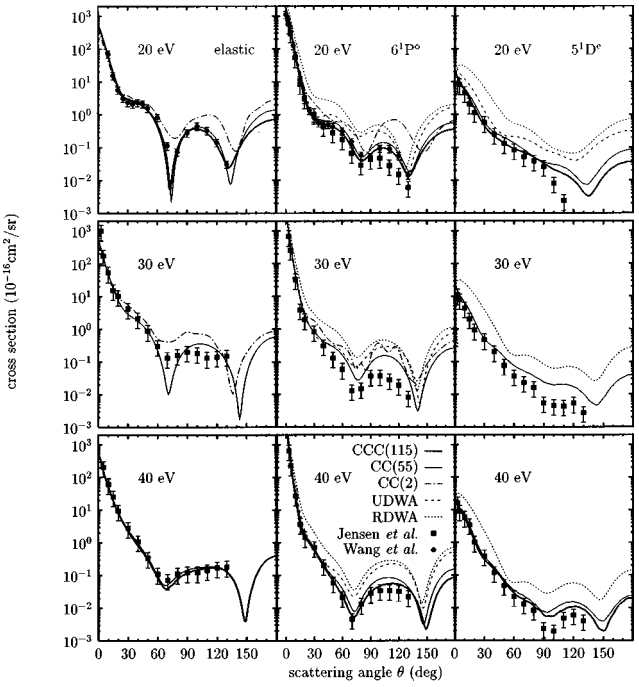

FIG. 10. The elastic, $6\,^1P^o$, and $5\,^1D^e$ excitation differential cross section for electron scattering on the Ba ground state at 20, 30, and 40 eV incident electron energy. CCC(115) and CC(55) calculations are described in the text. The UDWA calculations are due to Clark *et al.* [39], RDWA calculations are due to Srivastava *et al.* [40,41], and CC(2) calculations are due to Fabrikant [37]. Measurements are due to Wang, Trajmar, and Zetner [16] and Jensen, Register, and Trajmar [15].

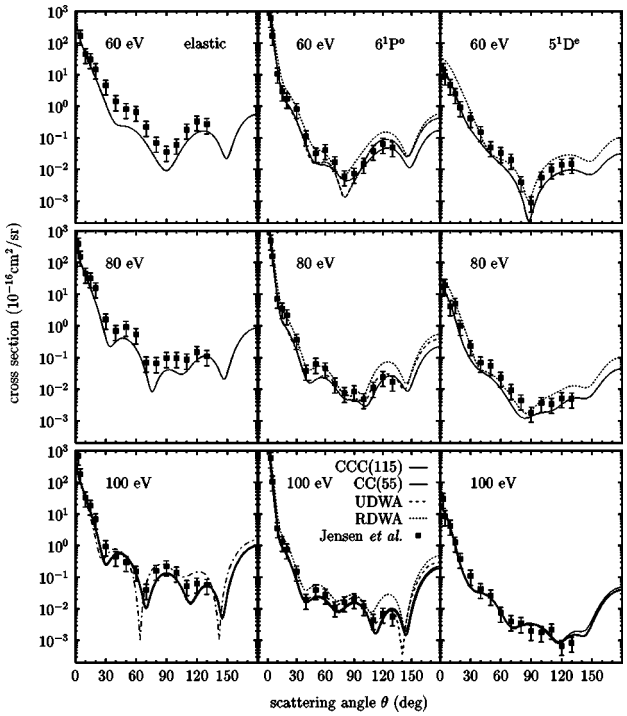

FIG. 11. The elastic, $6\,^1P^o$, and $5\,^1D^e$ excitation differential cross section for electron scattering on the Ba ground state at 60, 80, and 100 eV incident electron energy. Theoretical calculations are as in Fig. 10. In addition, the elastic DCS of Gregory and Fink [34] is also presented. Measurements are due to Jensen, Register, and Trajmar [15].

surements of Wang, Trajmar, and Zetner [16] and Jensen, Register, and Trajmar [15] have been normalized using Chen and Gallagher [14] $(6s6p)^1P^o$ apparent cross section as described above. Our elastic DCS is in excellent agreement with measurements of Wang, Trajmar, and Zetner [16] at 15 and 20 eV, and above 20 eV with data of Jensen, Register, and Trajmar [15]. Both CCC and CC(55) models give very much the same shape of the elastic DCS, indicating that coupling to the ionization channels do not affect elastic scattering significantly. The polarized-orbital calculations of Szmytkowski and Sienkiewicz [35] (not presented in Fig. 9) are in poor agreement with our calculations and experiment up to 80 eV, with relatively good agreement at 80 and 100 eV. At 100 eV, we have found very close agreement with calculation of elastic DCS by Gregory and Fink [34]. Note, that the CCC theory includes polarization effects and the calculations of Gregory and Fink do not. As a consequence there is more than 300% increase of the CCC elastic DCS over the results of Gregory and Fink at forward angles.

For $(6s6p)^1P^o$ DCS we observe that inclusion of the coupling to the target continuum in our CCC model reduced the CC(55) DCS uniformly while preserving the good shape-agreement with both sets of experimental data. At 20 eV, in the angular region of 90°–130°, where there is discrepancy between the two sets of $(6s6p)^1P^o$ DCS measurements, our results support the data of Wang, Trajmar, and Zetner [16]. For $(6s5d)^1D^e$ DCS we find, similarly to the previous case, that CCC(115) is below CC(55) and generally is in good agreement with experiment of Jensen, Register, and Trajmar [15]. At 20, 30, and 40 eV experimental data are somewhat below our calculations in the angular region 90°–130°, as in the 20 eV $(6s6p)^1P^o$ case.

The CC(2) calculations of Fabrikant [37] at 20 and 30 eV for elastic and $(6s6p)^1P^o$ DCS are in good agreement with experiment and our calculations at small scattering angles, but not at intermediate and large scattering angles. The UDWA [39,58] and RDWA [40,41] methods have been used to calculate $(6s6p)^1P^o$ and $(6s5d)^1D^e$ DCS. Below 60 eV (see Fig. 10) both methods substantially overestimate the excitation cross sections. Being based on the distorted-wave approximation, they are outside their energy range of validity. However, at 60 eV and above (see Fig. 11), we find good agreement with UDWA and RDWA results both in shape and absolute values of the DCS.

Elastic and $(6s6p)^1P^o$ DCS are highly peaked in the forward direction and their absolute normalization requires accurate measurement and extrapolation to very small angles. Disagreement between theoretical and measured or extrapolated experimental DCS at forward scattering angles, which have been noted before [39], brings additional uncertainty to the normalization of the experimental DCS. Renormalization of the experimental DCS, due to the difference in the estimate of the cascade contributions to the $(6s6p)^1P^o$ apparent cross section in the present work and in earlier experimental works together with reevaluation of the small angle behavior of the elastic and $(6s6p)^1P^o$ cross sections, would lead to a more accurate determination of the experimental normalization.

For the $(6s6p)^1P^o$ excitation the difficulties at small angles are highlighted by the transformation from the DCS to

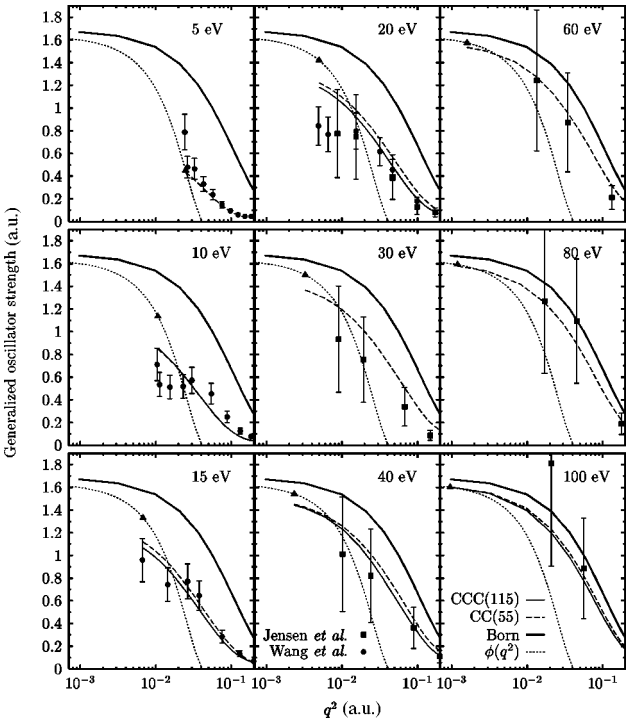

FIG. 12. Generalized oscillator strength for $6\,^1P^o$ excitation. Theoretical calculations and experiments as in Fig. 10, in addition the curve labeled $\phi(q^2)$ is the forward scattering function of Felfli and Msezane [59], with the $\theta=0°$ point at each energy marked by a triangle.

the generalized oscillator strength (GOS). In Fig.12 we compare our results with experimental data obtained from the $(6s6p)^1P^o$ DCS of Wang, Trajmar, and Zetner [16] and Jensen, Register, and Trajmar [15]. The curve labeled ''Born'' in Fig. 12 indicates the high-energy limit, and as $q\rightarrow 0$ converges to the (present theoretical) optical oscillator strength limit $f=1.69$ a.u. The close-coupling results CCC(115) and CC(55) are substantially below the Born limit at incident electron energies below 100 eV, which indicates that at these incident electron energies the first-order Born approximation is not yet valid. Note that a straightforward extrapolation of the theoretical or experimental GOS to zero q limit (optical f value) would result in an inaccurate value of the optical oscillator strength. At most of the presented energies in Fig. 12, experimental data are in good agreement with our results above approximately 5°, while at smaller angles they seems to experience some difficulties. This discrepancy at small scattering angles is of importance for correct absolute normalization of the relative DCS measurements using extrapolation of experimental GOS to optical f value or using method of integration over experimental DCS with normalization to the direct $(6s6p)^1P^o$ excitation cross section.

The matter of absolute normalization of the relative DCS measurements for barium $(6s6p)^1P^o$ excitation to the optical f value has been discussed recently by Felfli and Msezane [59]. They have used the forward scattering function $\phi(q^2)$ which describes the locus of the $\theta=0°$ GOS points at various incident electron energies. This function is presented in Fig. 12 and the $\theta=0°$ point is marked by the upper triangle on the $\phi(q^2)$ curve at each incident electron energy. Their

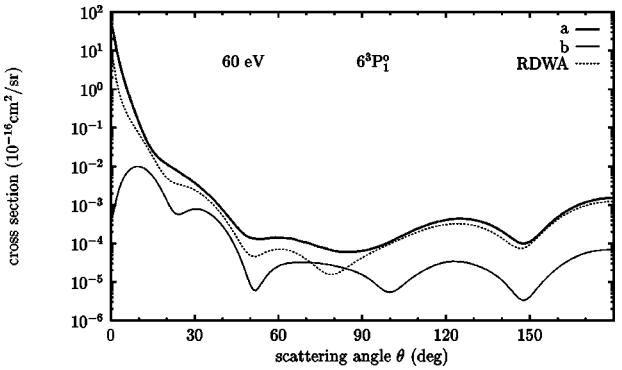

FIG. 13. The effect of singlet-triplet mixing on the $6\,^3P_1^o$ excitation differential cross section for electron scattering on the Ba ground state at 60 eV. Theoretical calculations: (a) CC(55) results with account of singlet-triplet mixing (see text for detail), (b) nonrelativistic CC(55) DCS for the $6\,^3P_1^o$ level, the RDWA calculation is due to Srivastava *et al.* [40].

idea is that experiment at each energy should be normalized to the $\phi(q^2)$ function at the zero scattering angle (marked by triangle). Comparing results of our CC(55) and CCC(115) calculations at $\theta=0°$ with corresponding values of the forward scattering function $\phi(q^2)$ we find agreement only at relatively large incident electron energies, at and above 80 eV. At smaller incident electron energies we find large discrepancies, the good agreement at 5 eV being purely coincidental. In particular, our results do not support the renormalization of the experimental data of Wang, Trajmar, and Zetner [16] at 10, 15, and 20 eV by factors of up to 2, as suggested by Felfli and Msezane [59].

No experimental data are available for the excitations of the Ba triplet states. Calculations in the RDWA methods have been reported for the 6^3P_1 state [40] and $5^3D_{1,2,3}$ states [41]. In the previous subsection we demonstrated the effect of the singlet-triplet mixing on the 6^3P_1 and 5^3D_2 ICS. As an example, we now examine its affect on the 6^3P_1 DCS at the incident electron energy of 60 eV. In the nonrelativistic approximation the relation of the DCS for excitation of a fine-structure sublevel J to the multiplet average DCS is given by Eq. (10). This CC(55) 6^3P_1 DCS and the RDWA calculation are presented in Fig. 13. The major difference is the forward angle behavior of the DCS. Nonrelativistic calculations predict the drop in the forward DCS, while relativistic calculations predict a sharp rise. The reason for this is the possibility of direct excitation of the 6^3P_1 level due to the presence of a singlet $6P$ component. We can account for the singlet-triplet mixing the same way as for the 6^3P_1 ICS. We use Eq. (11) for this purpose, and also present this result in Fig. 13. We obtain a fair agreement with the RDWA results. Note that at this energy both our and RDWA cross sections are dominated by the contribution from the singlet component, particularly for forward scattering. The difference between our and RDWA results in the forward direction is therefore caused by both the difference in the singlet-triplet mixing coefficients and the difference in the singlet $6P$ DCS. Taking into account that singlet $6P$ DCS in RDWA method is substantially larger than in our calculations, the singlet-triplet mixing coefficient in the RDWA model must be significantly smaller than the one we have used. We believe that our results should be more reliable due

to the close agreement with the experimental values for the optical oscillator strength of the intercombination $(6s6p)^3P_1^o$-$(6s^2)^1S$ line.

C. Electron-photon angular correlations for the $(6s6p)^1P^o$ state

We now present results of our calculations for the $(6s6p)^1P^o$ EICPs. The subject of electron-photon angular correlations have been reviewed extensively by Andersen, Gallagher, and Hertel [24]. We refer the reader to this reference for the details of the definitions of the presently used EICPs $L_\perp$, $P_\nearrow$, and γ, and to Ref. [6] for the details of calculation of the EICPs from the CCC scattering amplitudes.

Barium is a relatively heavy target and relativistic effects can affect the EICPs. These effects would be clearly seen as deviation of the degree of the total polarization P from unity. However, it was found both experimentally [28] and theoretically [39,40] that relativistic effects for the excitation of the $(6s6p)^1P^o$ state are negligible and P is very close to unity. This indicates that nonrelativistic LS coupling scheme is adequate for the description of the $(6s6p)^1P^o$ EICPs. In this case the collision process is fully coherent, and $P=\sqrt{L_\perp^2+P_\nearrow^2}=1$.

Another feature of the fully coherent $(6s6p)^1P^o$ excitation is the possibility, exploited by Li *et al.* [60], to determine parameter $\lambda=\mathrm{DCS}(m=0)/\mathrm{DCS}$, where $\mathrm{DCS}=\mathrm{DCS}(m=0)+2\,\mathrm{DCS}(m=1)$, directly from the superelastic scattering experiment. The parameter λ may also be expressed via the EICPs $\lambda=(P_\nearrow\cos2\gamma+1)/2$. It allows the determination of the magnetic sublevel $\mathrm{DCS}(m)$ if the DCS is also known. Magnetic sublevel $\mathrm{DCS}(m)$ are important for plasma diagnostic applications [61].

In Fig. 14 we compare our CCC(115) and CC(55) results for parameter λ with measurements of Li *et al.* [60] and the results of RDWA [40] and UDWA [39] calculations. We generally find close agreement between the CC(55) and CCC(115) calculations, indicating that coupling to the ionization continuum does not affect λ significantly. Similarly, we find agreement with the general angular behavior of the RDWA and UDWA results. Our results are in best agreement with experiment at 36.67 eV. At larger energies, 50 and 80 eV, our results are below experiment at scattering angles above 20°, where there are also large differences between the RDWA and UDWA results. Note that generally both RDWA and UDWA theories are in much better agreement with experiment for parameter λ than one would expect given their poor agreement with the corresponding DCS.

We now turn to Figs. 15 and 16, where theoretical and experimental EICPs $L_\perp$ and γ for the $(6s6p)^1P^o$ level are presented. Experimental data have been obtained using the superelastic scattering technique by Zetner, Li, and Trajmar [26,27] ($P_\nearrow$, γ) and Li and Zetner [28] ($L_\perp$). We used the relation between $L_\perp$ and $P_\nearrow$ to present Zetner, Li, and Trajmar data [26,27] for $P_\nearrow$ on the $L_\perp$ plot. Comparing with earlier theoretical results we observe that at 20 eV RWDA and UDWA are inadequate for the description of $L_\perp$. The results of the CC(2) calculation by Fabrikant [38] are in very close agreement with our results below 25° but are in poor agreement with both experiment and the present results at

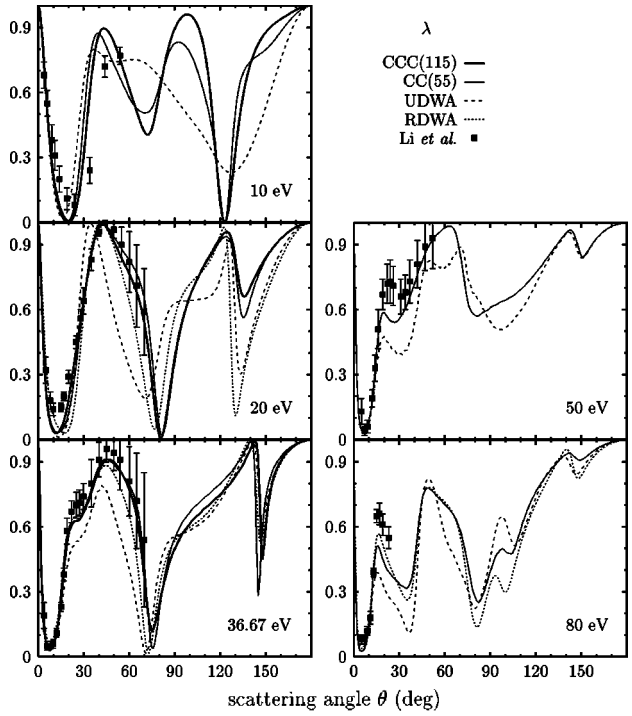

FIG. 14. Parameter λ for electron scattering on the Ba ground state at 36.67, 50, and 80 eV. Theoretical calculations are as for Fig. 10. Experiment is due to Li *et al.* [60].

larger scattering angles. The present calculations are in substantially better agreement with experiment for $L_\perp$ (and hence $P_\nearrow$) than the earlier calculations. In fact, for scattering angles above 30° the agreement is nearly perfect. However, for angles below 30° there is some discrepancy between different sets of measurements, with the close-coupling calculations favoring the data of Zetner, Li, and Trajmar [26]. The discrepancy between experiments [27,28] and present calculations for $L_\perp$ at small scattering angles can be due to influence of a finite scattering volume on the experimental data as discussed by Zetner, Trajmar, and Csanak [62]. However, this effect probably will not be sufficient to account for difference at 10°–30° interval.

Above 20 eV there is perfect agreement between all theoretical results and experiments at forward direction. At larger scattering angles we find very good agreement between all theories and experiment at 36.67 eV up to the largest experimental point at 92°, but at 50 eV some discrepancy develops between experiment and theoretical calculations around 60°, where the CCC results are in better shape agreement with experiment than the RDWA and UDWA results.

Given the differences between theoretical calculations and experiment for $L_\perp$, it is quite remarkable to find that for the parameter γ there is very close agreement between RDWA, UDWA, CCC, and experimental data. The calculation of Fabrikant (at 20 eV) also yields good agreement with γ, though in the case of $L_\perp$ agreement with experiment is only at small scattering angles. A number of experimental points reported in Ref. [27] have values of γ outside the (−90°, 90°) interval. In this case we present both the original value and the value transformed to the (−90°,90°) interval. For example, $\gamma=-99°$ is transformed to $\gamma=81°$.

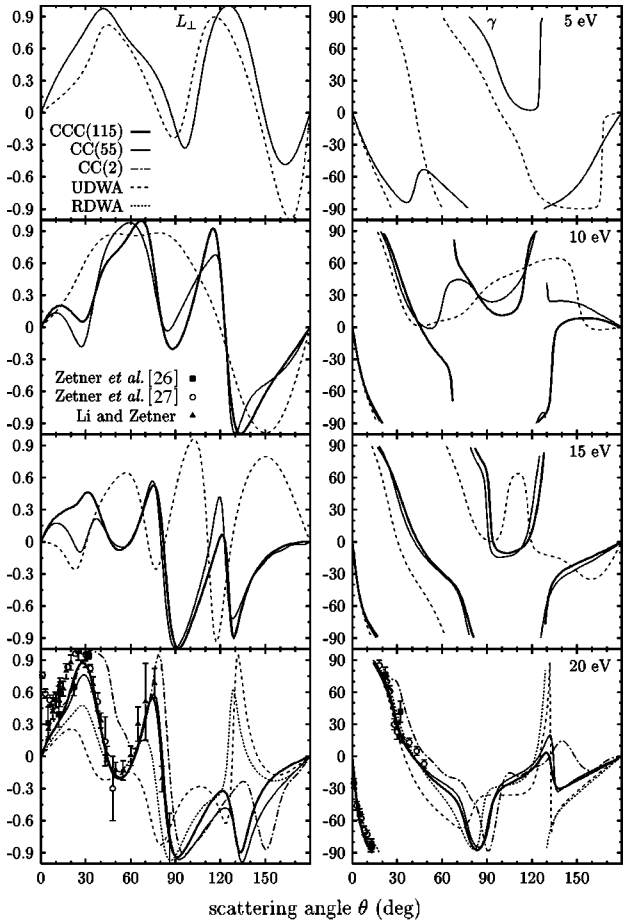

FIG. 15. EICPs $L_\perp$ and γ for electron scattering on the Ba ground state at 5, 10, 15, and 20 eV. Theoretical calculations are as for Fig. 10. Measurements are due to Zetner, Li, and Trajmar [26,27] and Li and Zetner [28].

In Fig. 15 we present EICPs $L_\perp$ and γ at low energies, of 5, 10, and 15 eV, where no measurements have been reported yet. We would like to attract attention to the radical change in the parameter $L_\perp$ as the energy decreases from 20 to 5 eV. Experimental investigation at this energy range may be of interest.

IV. CONCLUSIONS

We have extended the CCC method to the heaviest target yet, namely, the barium atom. The results of CCC(115) and CC(55) calculations have been compared with available experimental and theoretical data for electron scattering from the Ba ground state over a wide range of incident electron energies. Significant improvement has been found over earlier calculations, and in the case of integrated and differential cross section for elastic scattering and $(6s6p)^1P^o$ and $(6s5d)^1D^e$ excitations we have obtained essentially quantitative agreement with experimental data. We have also found that the present calculations are in good agreement with experiment for the $(6s6p)^1P^o$ EICPs, though some discrepancies are observed. Interestingly, the quality of agreement presented here for *e*-Ba scattering is the same as in the much simpler case of *e*-He scattering [10]. This suggests that, at least for the largest singlet-singlet cross sections, the nonrelativistic CCC theory is adequate for providing accurate results even for targets as heavy as barium.

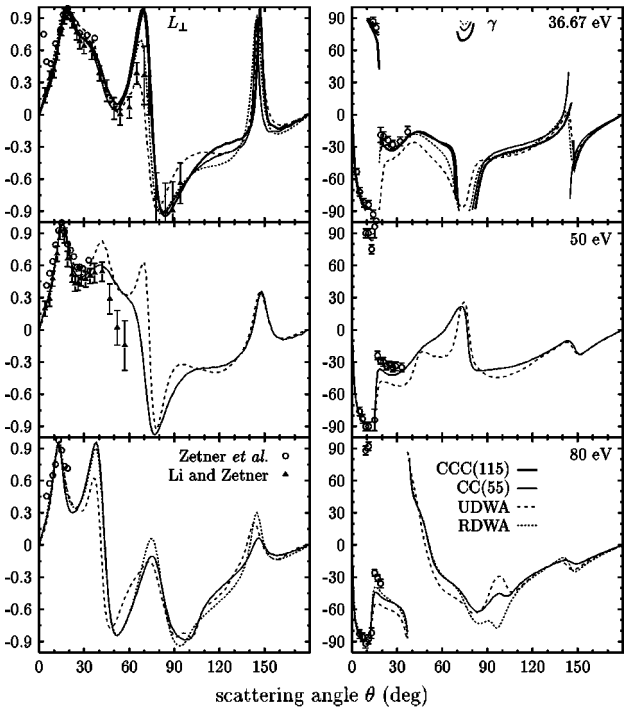

FIG. 16. EICPs $L_\perp$ and γ for electron scattering on Ba ground state at 36.67, 50, and 80 eV. Theoretical calculations are as for Fig. 10. Measurements are due to Zetner, Li, and Trajmar [27], and Li and Zetner [28].

We have also found that the nonrelativistic approximation fails for excitation of the $(6s6p)^3P_1^o$ and $(6s5d)^3D_2^e$ states, even though the spin-orbit interaction results in a relatively small singlet-triplet mixing coefficient. The way to remedy our results has been suggested. Experimental investigation of the triplet state excitations in Ba would be highly desirable to test the presented theoretical results.

Our result for the total ionization cross section (TICS) is systematically below the experimental data of Dettmann and Karstenssen [18], but in better agreement with data of Vainshtein *et al.* [17].

Even with the present nonrelativistic limitations, the CCC method has provided the most accurate to date *e*-Ba scattering results. The primary reason for this is its superior treatment of the electron scattering part of the calculations. Having established the validity and limitations of the CCC approach for electron scattering from the Ba ground state, we may confidently apply the theory to scattering from the excited states. We will also apply the CCC method to calculation of electron scattering from lighter alkaline earth atoms (Mg, Ca, Sr), where we expect the relativistic effects to be less important.

ACKNOWLEDGMENTS

We are grateful to George Csanak, Vladimir Kelemen, Al Stauffer, and Peter Zetner for communicating their data in electronic form. We would like to express our gratitude to Sandor Trajmar for helpful comments on the manuscript. Support of the Australian Research Council and the Flinders University of South Australia is acknowledged. We are also indebted to the South Australian Center for High Performance Computing and Communications.

[1] I. Bray and I. E. McCarthy, Phys. Rev. A **47**, 317 (1993).
[2] I. Bray and A. T. Stelbovics, Phys. Rev. A **46**, 6995 (1992).
[3] H. Yalim, D. Cvejanovic, and A. Crowe, Phys. Rev. Lett. **79**, 2951 (1997).
[4] R. W. O'Neill *et al.*, Phys. Rev. Lett. **80**, 1630 (1998).
[5] J. F. Williams, Aust. J. Phys. **51**, 633 (1998).
[6] D. V. Fursa and I. Bray, J. Phys. B **30**, 757 (1997).
[7] K. Bartschat, J. Phys. B **31**, L469 (1998).
[8] G. A. Piech *et al.*, Phys. Rev. A **55**, 2842 (1997).
[9] G. A. Piech, J. E. Chilton, L. W. Anderson, and C. C. Lin, J. Phys. B **31**, 859 (1998).
[10] D. V. Fursa and I. Bray, Phys. Rev. A **52**, 1279 (1995).
[11] D. V. Fursa and I. Bray, J. Phys. B **30**, 5895 (1997).
[12] V. Karaganov, I. Bray, P. J. O. Teubner, and P. Farrell, Phys. Rev. A **54**, R9 (1996).
[13] I. Bray, Phys. Rev. A **49**, 1066 (1994).
[14] S. T. Chen and A. Gallagher, Phys. Rev. A **14**, 593 (1976).
[15] S. Jensen, D. Register, and S. Trajmar, J. Phys. B **11**, 2367 (1978).
[16] S. Wang, S. Trajmar, and P. W. Zetner, J. Phys. B **27**, 1613 (1994).
[17] L. A. Vainshtein, V. I. Ochcur, V. I. Rakhovskii, and A. M. Stepanov, Sov. Phys. JETP **34**, 271 (1972).
[18] J. Dettmann and F. Karstensen, J. Phys. B **15**, 287 (1982).
[19] N. I. Romanyuk, O. B. Spernik, and I. P. Zapesochny, JETP Lett. **32**, 452 (1980).
[20] D. F. Register, S. Trajmar, S. W. Jensen, and R. T. Poe, Phys. Rev. Lett. **41**, 749 (1978).
[21] Y. Li and P. W. Zetner, Phys. Rev. A **49**, 950 (1994).
[22] P. W. Zetner *et al.*, J. Phys. B **30**, 5317 (1997).
[23] S. Trajmar *et al.*, J. Phys. B **31**, L393 (1998).
[24] N. Andersen, J. W. Gallagher, and I. V. Hertel, Phys. Rep. **165**, 1 (1988).
[25] Y. Li and P. W. Zetner, J. Phys. B **28**, 5151 (1995).
[26] P. W. Zetner, Y. Li, and S. Trajmar, J. Phys. B **25**, 3187 (1992).
[27] P. W. Zetner, Y. Li, and S. Trajmar, Phys. Rev. A **48**, 495 (1993).
[28] Y. Li and P. W. Zetner, Phys. Rev. A **49**, 950 (1994).
[29] E. M. Westcott *et al.*, Geophys. Res. Lett. **7**, 1037 (1980).
[30] D. J. Simons, M. B. Pongratz, G. M. Smith, and G. E. Barasch, J. Geophys. Res. **86**, 1576 (1981).
[31] S. A. Kazantsev and J. C. Henoux, *Polarization Spectroscopy of Ionized Gases* (Kluwer, Dordrecht, 1995).
[32] R. E. H. Clark, G. Csanak, J. Abdallah, and S. Trajmar, J. Phys. B **25**, 5233 (1992).
[33] P. V. Johnson, B. Eves, P. W. Zetner, D. Fursa, and I. Bray, Phys. Rev. A (to be published).
[34] D. Gregory and M. Fink, At. Data Nucl. Data Tables **14**, 39 (1974).
[35] R. Szmytkowski and J. E. Sienkiewicz, Phys. Rev. A **50**, 4007 (1994).
[36] I. I. Fabrikant, in *Atomnye Protsessy (Atomic Processes)*, edited by R. K. Peterkop (Zinatne, Riga, 1975), p. 80.
[37] I. I. Fabrikant, J. Phys. B **13**, 603 (1980).
[38] I. I. Fabrikant, Izv. Akad. Nauk Latv. SSR, Ser Fiz.Tekh. **6**, 11 (1985).
[39] R. E. Clark, J. Abdallah, Jr., G. Csanak, and S. P. Kramer, Phys. Rev. A **40**, 2935 (1989).
[40] R. Srivastava, T. Zuo, R. P. McEachran, and A. D. Stauffer, J. Phys. B **25**, 3709 (1992).
[41] R. Srivastava, R. P. McEachran, and A. D. Stauffer, J. Phys. B **25**, 4033 (1992).
[42] D. V. Fursa and I. Bray, Phys. Rev. A **57**, R3150 (1998).
[43] L. V. Chernysheva, N. A. Cherepkov, and V. Radojevic, Comput. Phys. Commun. **11**, 57 (1976).
[44] C. Laughlin and G. A. Victor, in *Atomic Physics*, edited by S. J. Smith and G. K. Walters (Plenum, New York, 1972), Vol. 3, pp. 247–255.
[45] D. W. Norcross and M. J. Seaton, J. Phys. B **9**, 2983 (1976).
[46] H. Friedrich and E. Trefftz, J. Quant. Spectrosc. Radiat. Transf. **9**, 333 (1969).
[47] S. Hameed, A. Herzenberg, and M. G. James, J. Phys. B **1**, 822 (1968).
[48] I. I. Sobel'man, *Introduction to the Theory of Atomic Spectra* (Pergamon Press, New York, 1972).
[49] C. W. Bauschlicher, Jr. *et al.*, J. Phys. B **18**, 2147 (1985).
[50] E. Trefftz, J. Phys. B **7**, L342 (1974).
[51] B. M. Miles and W. L. Wiese, At. Data **1**, 1 (1969).
[52] T. M. Miller and B. Bederson, Adv. At. Mol. Phys. **13**, 1 (1977).
[53] P. G. Burke and W. D. Robb, Adv. At. Mol. Phys. **11**, 143 (1975).
[54] K. Bartschat *et al.*, J. Phys. B **29**, 115 (1996).
[55] Y.-K. Kim and P. S. Bagus, Phys. Rev. A **8**, 1739 (1973).
[56] V. I. Kelemen, E. Y. Remeta, and E. P. Sabad, J. Phys. B **28**, 1527 (1995).
[57] I. Bray, Phys. Rev. Lett. **73**, 1088 (1994).
[58] G. Csanak (private communication).
[59] Z. Felfli and A. Z. Msezane, J. Phys. B **31**, L165 (1998).
[60] Y. Li, S. Wang, P. W. Zetner, and S. Trajmar, J. Phys. B **27**, 4025 (1994).
[61] S. A. Kazantsev, N. Polynovskaya, L. N. Pyatnitskii, and S. A. Edel'man, Sov. Phys. Usp. **31**, 785 (1988).
[62] P. W. Zetner and S. T. G. Csanak, Phys. Rev. A **41**, 5980 (1990).
[63] C. E. Moore, *Atomic Energy Levels*, Natl. Bur. Stand. (U.S.) Circ. No. 467 (U.S. GPO, Washington, DC, 1949), Vol. III.
[64] H. P. Palenius, Phys. Lett. **56A**, 451 (1976).
[65] W. H. Parkinson, E. M. Reeves, and F. S. Tomkins, J. Phys. B **9**, 157 (1976).
[66] E. Hulpke, E. Paul, and W. Paul, Z. Phys. **177**, 257 (1964).
[67] J. Brecht *et al.*, Z. Phys. **264**, 273 (1973).
[68] A. F. Bernhardt, D. E. Duerre, J. R. Simpson, and L. L. Wood, J. Opt. Soc. Am. **66**, 416 (1976).
[69] L. Jahreiss and M. C. E. Huber, Phys. Rev. A **28**, 3382 (1983).
[70] H. Harima, T. Yoshida, and Y. Urano, J. Phys. Soc. Jpn. **45**, 357 (1978).
[71] H. F. Eicke, Z. Phys. **168**, 227 (1962).
[72] P. McCavert and E. Trefftz, J. Phys. B **7**, 1270 (1974).